Open Access **Baghdad Science Journal** **P-ISSN: 2078-8665**
Published Online First: January 2022 **2022, 19(4): 914-921** **E-ISSN: 2411-7986**

DOI: http://dx.doi.org/10.21123/bsj.2022.19.4.0914

Investigation of the Nuclear Structure of Some Ni and Zn Isotopes with Skyrme-Hartree-Fock Interaction

Shaimaa A. Abbas* ***Seham Hassan Salman*** ***Samira A. Ebrahiem***
Huda M. Tawfeek

Department of Physics, College of Education for Pure Science (Ibn-Alhaitham), University of Baghdad, Baghdad, Iraq.
*Corresponding author: shaimaa19750@gmail.com
E-mail address: seham.h.s@ihcoedu.uobaghdad.edu.iq, sameera.a.i@ihcoedu.uobaghdad.edu.iq, hudamtawfeek@gmail.com

Received 19/6/2021, Accepted 31/8/2021, Published Online First 20/1/2022, Published 1/8/2022

Abstract:

The inelastic C2 form factors and the charge density distribution (CDD) for ^{58,60,62}Ni and ^{64,66,68}Zn nuclei has been investigated by employing the Skyrme-Hartree-Fock method with (Sk35-Skzs*) parametrization. The inelastic C2 form factor is calculated by using the shape of Tassie and Bohr-Mottelson models with appropriate proton and neutron effective charges to account for the core-polarization effects contribution. The comparison of the predicted theoretical values was conducted with the available measured data for C2 and CDD form factors and showed very good agreement.

Keywords: Charge density distribution (CDD), C2 form factors, Skyrme-Hartree-Fock, Shell model

Introduction:

In order to know the nuclear forces and the laws that govern the interactions between elementary particles, the only possible method is that of scattering a diversity of particles by a diversity of targets. There will be three types of scattering experiments, the first one is that the incident particle has no atomic force, but interacts with the nucleus via only electromagnetic interaction, such as speedy electron scattering. The data on charge and current densities can be given[1]. Secondly, the scattering of neutral electrical particles, for example neutrons that only contribute to nuclear fields. Lastly, the scattering of particles charged by electricity, oftentimes experiences strong nuclear contact such as proton and alpha particle. The scattering of nuclear electrons provides the most detailed knowledge about the nuclear size and distribution of charge and offers valuable information about electromagnetic currents within nuclei. Electron scattering can be a good test for calculation because it is sensitive to spatial load dependency and current densities[2,3]. To explain nuclei using the nuclear shell model, one must understand the effective one- and two-body interactions. Several techniques for calculating the effective interaction for nuclei in the fp-shells have been proposed in the last 30 years[4]. Kuo and Brown proposed the first comprehensive technique in the 1960s, using the Hamada-Johnston potential[5]. In model space calculations, Radhi et al[6-9] showed that it is advisable to include CP effect in form-factors for nuclei in the beginning of p-shell and the end of sd-shell. F. A. Majeed et al [10-12] demonstrated that form factor calculations based on large-basis of the shell model to study the nuclei in the p, sd and fp shells considering the contribution of high-energy configurations beyond the p, sd and fp shell space model space denoted as the core polarization effects. The proton and neutron matter density distribution and their related charge radii along with the ground state form factors have been investigated by Hameed BS[13] for some selected potassium isotopes, their conducted study showed that taking into consideration the core polarization effects along with effective g-factors made remarkable enhancement in their calculations which leads to good agreement with the measured data.

The recent developments with new modern effective interactions designed for fp-shell region are still not universal and need more tuning. The nuclei at the upper limit of the fp-shell region attract attention in recent years due to their importance in

understanding the supernova explosions, therefore this study aimed to investigate the charge density distribution (CDD) and the inelastic C2 form factors for ^{58,60,62}Ni and ^{64,66,68}Zn nuclei by employing the Skyrme-Hartree-Fock method with (Sk35-Skzs*) parametrization and comparing he predicted theoretical calculations with the available measured data.

Theoretical Background

Skyrme Effective Interaction

Skyrme presented an effective interaction for HF calculations of nuclei[14,15]. In describing the ground conditions properties of nuclei with approximately ten adjustable parameters, it is the more convenient force used to fit experimental nuclei data such as binding energies and charged radii[16]. The Skyrme forces are zero-range interactions that are composed of a momentum-dependent two-body term and a zero-range three-body term. A density-dependent two-body term can be replaced for the three-body term in the HF calculations. As a result, as an extended Skyrme force[17], the Skyrme forces are unified in a single form. The interaction between two bodies in Skyrme is written as follows[14]:

$$\begin{aligned} v_{12} = {} & t_0\left(1 + x_0\hat{P}_\sigma\right)\delta(\vec{r}_1 - \vec{r}_2) \\ & + \frac{t_1}{2}\left(1 + x_1\hat{P}_\sigma\right)\left(\hat{k}^2\delta(\vec{r}_1 - \vec{r}_2)\right. \\ & \left. + \delta(\vec{r}_1 - \vec{r}_2)\hat{\acute{k}}^2\right) \\ & + t_2\left(1 + x_2\hat{P}_\sigma\right)\hat{\acute{k}}.\delta(\vec{r}_1 - \vec{r}_2)\hat{k} \\ & + \frac{t_3}{6}\left(1 + x_3\hat{P}_\sigma\right)\rho^\alpha\left(\vec{R}\right)\delta(\vec{r}_1 - \vec{r}_2) \\ & + iW_0\hat{\acute{k}}(\hat{\sigma}_1 + \hat{\sigma}_2) \\ & \times \hat{k}\delta(\vec{r}_1 - \vec{r}_2) \quad \ldots\ldots\ldots \quad 1 \end{aligned}$$

here $\vec{\boldsymbol{R}} = \frac{\vec{\boldsymbol{r}}_1 + \vec{\boldsymbol{r}}_2}{2}$ and $\boldsymbol{\alpha}$ is the parameters of Skyrme force. The $\hat{\boldsymbol{k}} = \left(\vec{\boldsymbol{\nabla}}_1 - \vec{\boldsymbol{\nabla}}_2\right)/2\boldsymbol{i}$ and $\hat{\acute{\boldsymbol{k}}} = -\left(\overleftarrow{\boldsymbol{\nabla}}_1 - \overleftarrow{\boldsymbol{\nabla}}_2\right)/2\boldsymbol{i}$ operators are the relative momentum wave vectors of two nucleons acts to the right and to the left (i.e., the complex conjugate wavefunctions, with coordinate $\acute{\boldsymbol{r}}$ respectively. The terms $\boldsymbol{t_0}$, $\boldsymbol{t_1, t_2, t_3, x_1, x_2, x_3}$ and $\boldsymbol{W_0}$ are free parameters that describe the strengths of various interaction factors that are fitted to nuclear structure data. $\hat{\boldsymbol{\sigma}}$ is the Pauli matrices, $\hat{\boldsymbol{P}}_{\boldsymbol{\sigma}} = \frac{\boldsymbol{1}}{\boldsymbol{2}}\left(\boldsymbol{1} + \hat{\boldsymbol{\sigma}}_{\boldsymbol{1}} \cdot \hat{\boldsymbol{\sigma}}_{\boldsymbol{2}}\right)$ is operator of spin-exchange, and the Dirac delta function $\boldsymbol{\delta}(\vec{\boldsymbol{r}}_{\boldsymbol{1}} - \vec{\boldsymbol{r}}_{\boldsymbol{2}})$. In the typical Skyrme–Hartree–Fock (SHF) model, the total energy density of a nucleus is expressed as[14]

$$E = E_{kin} + E_{Sky} + E_{Coul} + E_{pair} - E_{cm} \quad \ldots\ldots 2$$

$\boldsymbol{E_{kin}}$ is the kinetic energy of the nucleons (proton and neutron) can be calculated using the following formula[15]

$$E_{kin} = \sum_{i=1}^{A} \frac{\hbar^2}{2m_i} \int \tau_i d^3r \quad \ldots\ldots 3$$

$\boldsymbol{E_{sky}}$ is the energy functional of the Skyrme force and given by[15],

$$\begin{aligned} E_{sky} = \int d^3r \Bigg[& \frac{b_0}{2}\rho^2 - \frac{\acute{b}_0}{2}\sum_q \rho_q^2 + \frac{b_3}{3}\rho^{\alpha+2} \\ & - \frac{\acute{b}_3}{3}\rho^\alpha \sum_q \rho_q^2 + b_1\tau_q \\ & - \acute{b}_1 \sum_q \rho_q\tau_q - \frac{b_2}{2}\rho\Delta\rho \\ & + \frac{\acute{b}_2}{2}\sum_q \rho_q\Delta\rho_q - b_4\rho\nabla.J \\ & - \acute{b}_4 \sum_q \rho_q\nabla.J_q \Bigg] \quad \ldots\ldots 4 \end{aligned}$$

ρ_q is the local densities for protons and neutrons (depending on the value of q), ρ is the total density, τ_q is the kinetic energy densities for protons and neutrons and J_q is the spin-orbit current density. They are given by these relations[15]

$$\begin{aligned} & \rho_q(r) = \textstyle\sum_{i\sigma}|\phi_i(r,\sigma,q)|^2, \\ & \tau_q(r) = \textstyle\sum_{i\sigma}\left|\vec{\nabla}\phi_i(r,\sigma,q)\right|^2, \\ & J_q(r) = -i\sum_{i\sigma\acute{\sigma}} \phi_i^*(r,\sigma,q)[\nabla\phi_i \times \langle\sigma|\hat{\sigma}|\acute{\sigma}\rangle] \quad \ldots\ldots 5 \end{aligned}$$

The below are the parameters in the energy Skyrme equation[15,16]

$$\begin{aligned} & b_0 = t_0\left(1 + \tfrac{1}{2}x_0\right), \acute{b}_0 = t_0\left(\tfrac{1}{2} + x_0\right) \\ & b_1 = \tfrac{1}{4}\left[t_1\left(1 + \tfrac{1}{2}x_1\right) + t_2\left(1 + \tfrac{1}{2}x_2\right)\right], \acute{b}_1 = \\ & \tfrac{1}{2}\left[t_1\left(\tfrac{1}{2} + x_1\right) - t_2\left(\tfrac{1}{2} + x_2\right)\right] \\ & b_2 = \tfrac{1}{8}\left[3t_1\left(1 + \tfrac{1}{2}x_1\right) - t_2\left(1 + \tfrac{1}{2}x_2\right)\right], \acute{b}_2 = \\ & \tfrac{1}{8}\left[3t_1\left(\tfrac{1}{2} + x_1\right) + t_2\left(\tfrac{1}{2} + x_2\right)\right] \\ & b_3 = \tfrac{1}{4}t_3\left(1 + \tfrac{1}{2}x_3\right), \acute{b}_3 = \tfrac{1}{4}t_3\left(\tfrac{1}{2} + x_3\right) \quad \ldots\ldots 6 \end{aligned}$$

The nucleon densities $\rho_\rho(r)$ and $\rho_n(r)$ may be calculated from a single particle wave function defined by the HF calculation. In the (SHF) theory using the Skyrme forces, the most general product wave functions (ψ_β) consist of independently moving single particles. In this method the neutron and proton densities are given in

$$\rho_q(\vec{r}) = \sum_i |\varphi_i(r)|^2 = \sum_\beta \omega_\beta \frac{2j_\beta + 1}{4\pi}\left(\frac{R_\beta}{r}\right)^2 \quad \ldots. 7$$

where β represents the state, ω_β is the probability of the state, and j_β the angular momentum of the state. The Coulomb energy part is the third part of the total energy equation. The exchange component contributes a modest amount of energy to the Coulomb energy. This contribution is owing to the fact that the Coulomb interaction is infinite range. The Coulomb energy is calculated as follows [15,17]:
where R_β is the radial part of the harmonics oscillator wavefunction and is given as

$$R_\beta = \sqrt{\frac{2n!}{b^3\,\Gamma\left(n+l+\frac{3}{2}\right)}}\left(\frac{r}{b}\right)^l e^{-r^2/2b^2}\; L_n^{\left(l+\frac{1}{2}\right)}\left(\frac{r^2}{b^2}\right) \quad \ldots\ldots\ldots 8$$

where $L_n^{\left(l+\frac{1}{2}\right)}$ is the associated Laquerre polynomials and b is the harmonic oscillator size parameter.

$$E_{Coul} = \frac{e^2}{2}\iint \frac{\rho_q(\vec{r})\rho_q(\vec{\acute{r}})}{\left|\vec{r}-\vec{\acute{r}}\right|} d^3r d^3\acute{r} + E_{Coul,exch} \quad \ldots\ldots\ldots 9$$

$$E_{Coul,exch} = -\frac{3}{4}e^2\left(\frac{3}{\pi}\right)^{1/3}\int \rho^{4/3}{}_q(\vec{r})\, d\vec{r} \quad \ldots. 10$$

$$E_{coul,exch} = -\frac{\langle P_{cm}^2\rangle}{2\,A\,m} \quad \ldots\ldots\ldots 11$$

where $P_{cm} = \sum_i \hat{p}_i$ is the total momentum operator, A the nucleon number and m the average nucleon mass.

Tassie and Bohr-Mottelson

The Tassie model (TM) used in NushellX@MSU[18] for core polarization is a more elastomeric and modified modeling that allows for a non-uniform mass and charge density distribution. In the TM model, the CP charge density is determined by the nucleus ground state charge density. The two-body charge density for all occupied shells, including the core, has been used to obtain the ground state charge density. The Tassie shape core polarization transition density, which is based on the collective modes of the nuclei is given by[19]

$$\rho_{Jt_z}^{core}(i,f,r) = \frac{1}{2}C(1+\tau_z)\, r^{J-1}\frac{d\rho_0(i,f,r)}{dr} \quad \ldots\ldots 12$$

where C is a constant of the proportionality and ρ_0 is the charge density distribution for the ground state two-body, which is given[20],

$$\rho_0 = \left\langle\psi\left|\hat{\rho}_{eff}^{(2)}(\vec{r})\right|\psi\right\rangle = \sum_{i<j}\left\langle ij\left|\hat{\rho}_{eff}^{(2)}(\vec{r})\right|ij\right\rangle - \left\langle ij\left|\hat{\rho}_{eff}^{(2)}(\vec{r})\right|ji\right\rangle \quad \ldots\ldots 13$$

where,

$$\hat{\rho}_{eff}^{(2)}(\vec{r}) = \frac{1}{2(A-1)}f(r_{ij})\sum_{i\neq j}\left\{\delta(\vec{r}-\vec{r_i}) + \delta(\vec{r}-\vec{r_j})\right\}f(r_{ij}) \quad \ldots. 14$$

where i and j are all the required quantum numbers, i.e., the functions $f(r_{ij})$ are the two-body short range correlation (SRC). In this work, a simple model form of short-range correlation has been adopted[20], i.e.,

$$f(r_{ij}) = 1 - \exp\left[-\beta\left(r_{ij}-r_c\right)^2\right] \quad \ldots\ldots 15$$

where r_c is the suitable hard core radius and β is a parameter of the correlation. For this model the Coulomb form factor becomes[20]:

$$F_J^L(q) = \sqrt{\frac{4\pi}{2J_i+1}}\frac{1}{Z}\left\{\int_0^\infty r^2 j_J(qr)\rho_{Jt_z}^{ms}(i,f,r)\, dr + C\int_0^\infty j_J(qr)\, r^{J+1}\frac{d\rho_0(i,f,r)}{dr}dr\right\} F_{cm}(q)\, F_{fc}(q) \ldots. 16$$

but,

$$\int_0^\infty j_J(qr)\, r^{J+1}\frac{d\rho_0(i,f,r)}{dr}dr = \int_0^\infty \frac{d}{dr}\left[j_J(qr)\, r^{J+1}\rho_0(i,f,r)\right]dr - \int_0^\infty (J+1)\, j_J(qr)\, r^J\rho_0(i,f,r)\, dr - \int_0^\infty \frac{d\, j_J(qr)}{dr}\, r^{J+1}\rho_0(i,f,r)\, dr \quad \ldots\ldots 17$$

where the first term gives zero contribution, the second and the third term can be combined together as[19],

$$-q\int_0^\infty r^{J+1}\rho_0(i,f,r)\left[\frac{d}{d(qr)} + \frac{J+1}{qr}\right]j_J(qr)\, dr \quad \ldots. 18$$

from the recursion of the spherical Bessel function[17],

$$\left[\frac{d}{d(qr)}+\frac{J+1}{qr}\right]j_J(qr) = j_{J-1}(qr) \quad \ldots\ldots\ldots 19$$

$$\therefore \int_0^\infty j_J(qr)\, r^{J+1}\frac{d\rho_0(i,f,r)}{dr}dr = -q\int_0^\infty r^{J+1}\rho_0(i,f,r)\, j_{J-1}(qr)\, dr \quad \ldots\ldots 20$$

Therefore, the form factor of eq.(14) takes the form[20]:

$$F_J^L(q) = \sqrt{\frac{4\pi}{2J_i+1}}\frac{1}{Z}\left\{\int_0^\infty r^2 j_J(qr)\rho_{Jt_z}^{ms}(i,f,r)\, dr$$

$$-qC\left\{\int_0^\infty r^{J+1}\rho_0(i,f,r)\,j_{J-1}(qr)\,dr\right\}F_{cm}(q)\,F_{fc}(q) \quad \ldots. 21$$

The constant of the proportionality C can be determined from the form factor evaluated at $q = k$, i.e. substituting $q = k$ in above equation we obtained[19],

$$C = \frac{\int_0^\infty r^2 j_J(kr)\rho^{ms}_{J\,t_z}(i,f,r)\,dr - ZF^L_J(k)\sqrt{\frac{2J_i+1}{4\pi}}}{\int_0^\infty r^{J+1}\rho_0(i,f,r)\,j_{J-1}(kr)\,dr} \quad \ldots\ldots 22$$

Results and Discussion:

There are many theoretical tools available to describe the properties of fp-shell nuclei that are available. Such calculations vary with the completion of the space of the shell model, the mass dependent of the involved parameters and the two-matrix elements is appropriate in terms of experimental results, in the present work ^{58,60,62}Ni and ^{64,66,68}Zn. The jun45 interaction has been used to give the $1f_{5/2}2p_{1/2}1g_{9/2}$-shell model wave functions. The core is taken as ^{56}Ni for all the nuclei under study with different valence neutrons for Ni isotopes and two valence protons with different values of valence neutrons for Zn isotopes. The Bohr-Mottelson and Tassie models were employed to perform the present calculations. The curve with red dots displays the results of the calculations Tassie in any of the following diagrams (see Fig.1). The Bohr-Mottelson calculations are shown by the solid blue curve.

The parameters used with Sk35-Skzs* used to perform the calculations are listed in Table1.

Table 1. The Skyrme parameterization which is adopted in the calculations

Force	Sk35-Skzs*
t_o (MeV.fm^3)	-1446.759
t_1 (MeV.fm^3)	250.852
t_2 (MeV.fm^3)	-132.993
t_3 (MeV.fm^3)	12127.649
W_o	153.054
x_o	0.329
x_1	0.518
x_2	0.139
x_3	0.018
α	1/2

^{58,60,62}Ni Isotopes

The shell model calculations have been performed by adopting the model space jj44 with core at ^{56}Ni, therefore we have 2, 4 and 6 valence neutrons for ^{58}Ni, ^{60}Ni, and ^{62}Ni, respectively. The longitudinal form factor C2 for the state $(J^\pi T = 2_1^+ 1)$ of ^{58}Ni nucleus in fp-shell is presented in Fig. 1. The effective interaction jun45 is utilized as effective interaction for the calculations of the shell model and the (Sk35-Skzs*) residual interaction to calculate the matrix element for the interactions from initial to final states. The first maxima are very well reproduced by both Tassie Model and Bohr-Mottelson calculations. The second maxima did not agree in comparison with the calculations. The experimental data for this state is taken from Ref.[21]. The effective proton and neutron charges used in these calculations are 0.5 and 1.5, respectively. Figure 2. shows the CDD obtained with the investigated Skyrme parameterization Sk35-Skzs* used in this work as well as the experimental charge distributions for ^{58}Ni nucleus**.** Theoretically the calculated CDD is quite consistent with the theoretical calculations with the Skyrme parameterization.

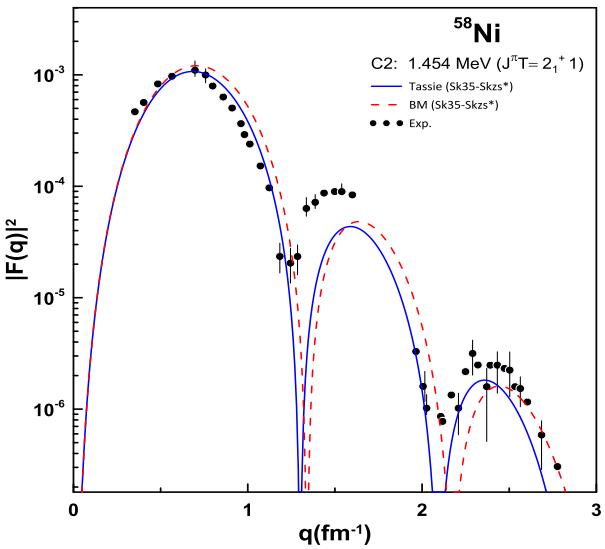

Figure 1. C2 form factor for the 2_1^+1 state in ^{58}Ni. Measured data from[21].

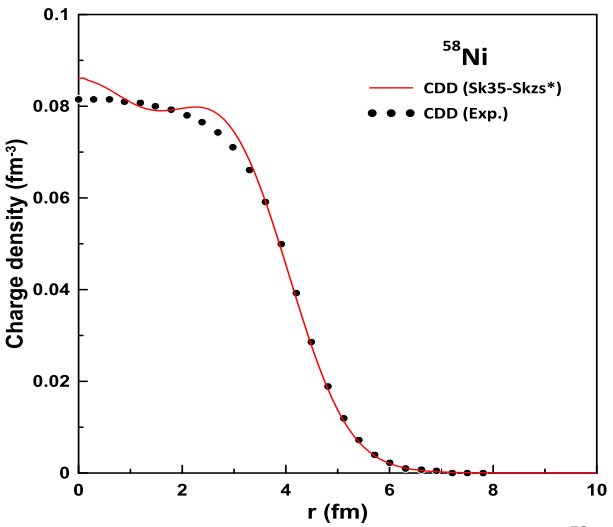

Figure 2. Charge density distribution for ^{58}Ni using Skyrme parameterization "Sk35-Skzs*". Measured data from[21].

The C2 longitudinal form factor for the state $(J^{\pi}\ T = 2_1^+2)$ of ^{60}Ni nucleus has been calculated by Tassie model and Bohr-Mottelson models. The calculations according to standard shell model the core is taken at ^{56}Ni with four neutrons as valence particles outside the core, as shown in Fig. 3. The core polarization is considered by using the effective proton and neutron charges. Figure 4 shows the CDD obtained with the investigated Skyrme parameterization Sk35-Skzs*used in this work as well as the experimental charge distributions for ^{60}Ni nucleus**.** The comparison of the predicted theoretical values was compared with the available measured data for CDD and C2 form factors and showed good agreement.

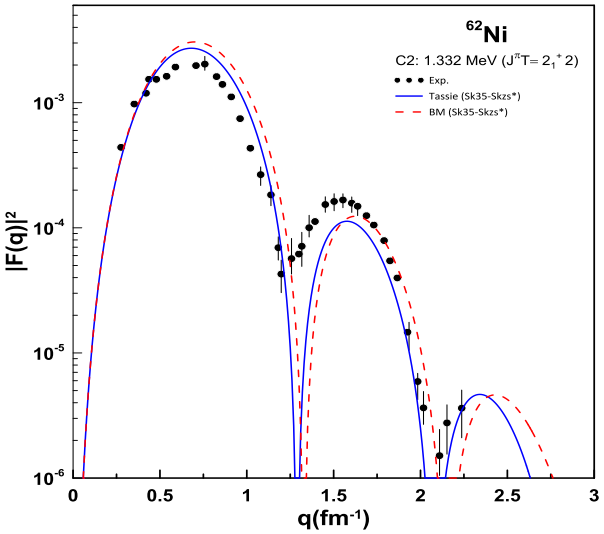

Figure 3. C2 form factor for the 2_1^+2 state in ^{60}Ni. Measured data from[21].

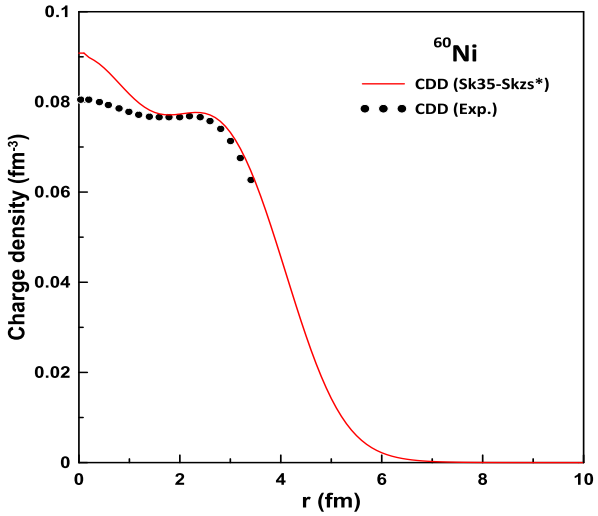

Figure 4. Charge density distribution for ^{60}Ni using Skyrme parameterization "Sk35-Skzs*". Measured data from[21].

The nucleus ^{62}Ni excites in this transition from ground state $(J_i^{\pi}\ T = 0_1^+3)$ to the excited state $(J_f^{\pi}\ T = 2_1^+3)$ with the corresponding energy 1.172 MeV. The C2 longitudinal form factor of ^{62}Ni nucleus in $1f_{5/2}2p_{1/2}1g_{9/2}$-shell is presented in Fig. 5. The jun45 is utilized as an effective residual interaction for the calculations of the shell model. The third maxima are very well reproduced by both Tassie and Bohr-Mottelson calculations. The experimental data for this state are taken from Ref.[23]. Figure 6 shows the CDD obtained with the investigated Skyrme parameterization Sk35-Skzs* used in this work as well as the experimental charge distributions for ^{62}Ni nucleus **.**The comparison of the predicted theoretical values was compared with the available measured data for CDD and C2 form factors and showed good agreement.

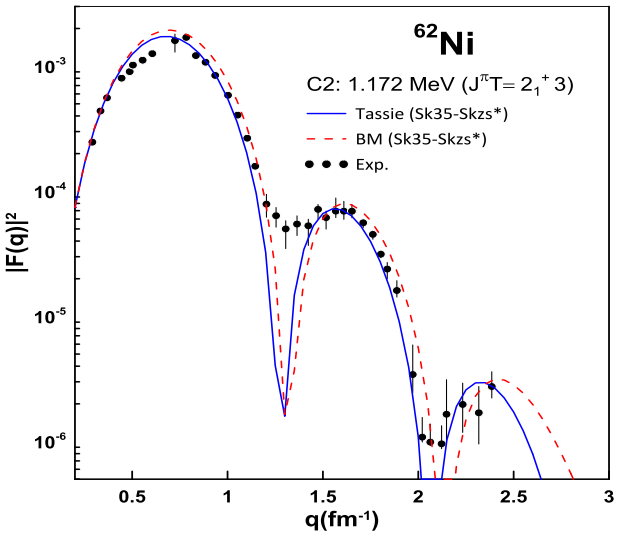

Figure 5. C2 form factor for the 2_1^+3 state in ^{62}Ni. Measured data from[22].

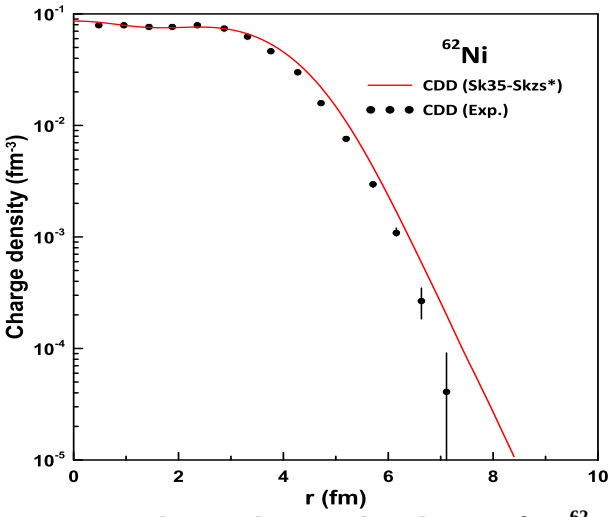

Figure 6. Charge density distribution for ^{62}Ni using Skyrme parameterization "Sk35-Skzs*". Measured data from[22].

^{64,66,68}Zn Isotopes

The shell model calculations for Zn isotopes have been performed by considering the jj44 model space which assumes ^{56}Ni as core with 2 protons and 6, 8 and 10 neutrons outside the core for ^{64}Zn, ^{66}Zn, and ^{68}Zn, respectively. The C2 longitudinal form factor for ^{64,66,68}Zn isotopes have been calculated in Figs.7,8,9 respectively by Tassie model and Bohr-Mottelson models. The effective interaction jun45 is utilized as effective interaction for the calculations of the shell model and the (Sk35-Skzs*) residual interaction to calculate the matrix element for the interactions from initial to final states. The experimental data was reproduced by both Tassie Model and Bohr-Mottelson calculations for the ^{64,66,68}Zn isotopes. The experimental data for this state was aken from Ref.[22]. The effective proton and neutron charges used in these calculations are 0.5 and 1.0, respectively. Figures 10,11,12. show the CDD obtained with the investigated Skyrme parameterization Sk35-Skzs*used in this work as well as the experimental charge distributions for ^{64,66,68}Zn isotope. The comparison of the predicted theoretical values was compared with the available measured data for CDD and C2 form factors and showed good agreement.

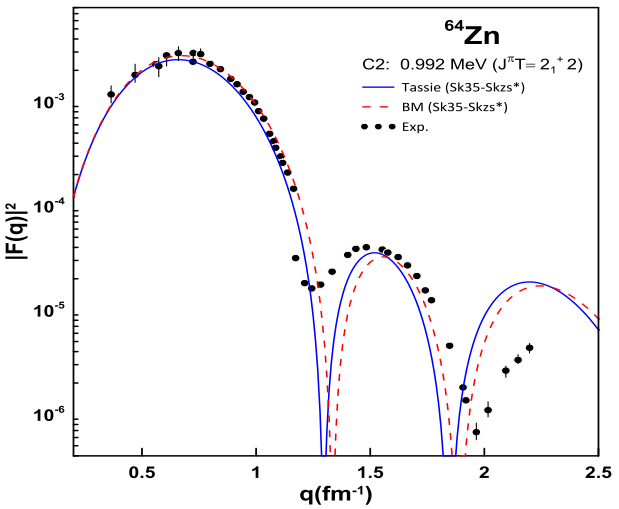

Figure 7. C2 form factor for the 2_1^+2 state in ^{64}Zn. Measured data from[23].

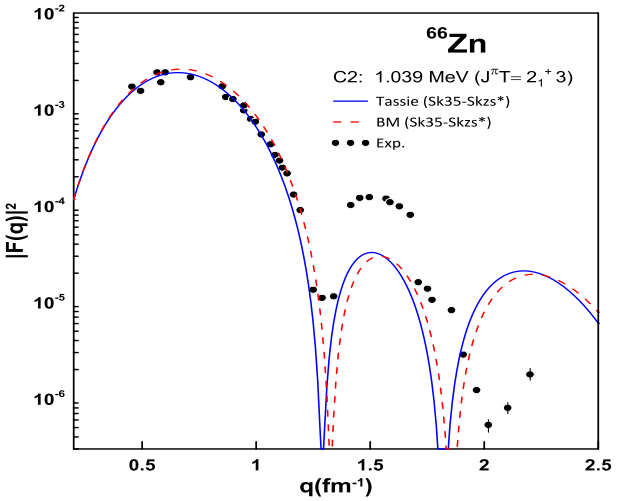

Figure 8. C2 form factor for the 2_1^+3 state in ^{66}Zn. Measured data from[22].

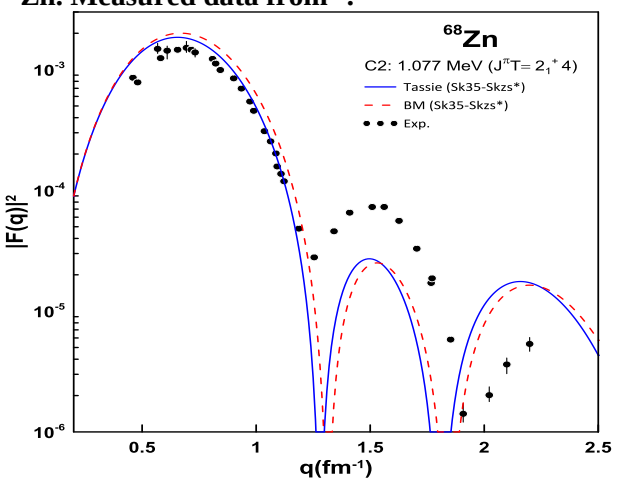

Figure 9. C2 form factor for the 2_1^+4 state in ^{68}Zn. Measured data from[22].

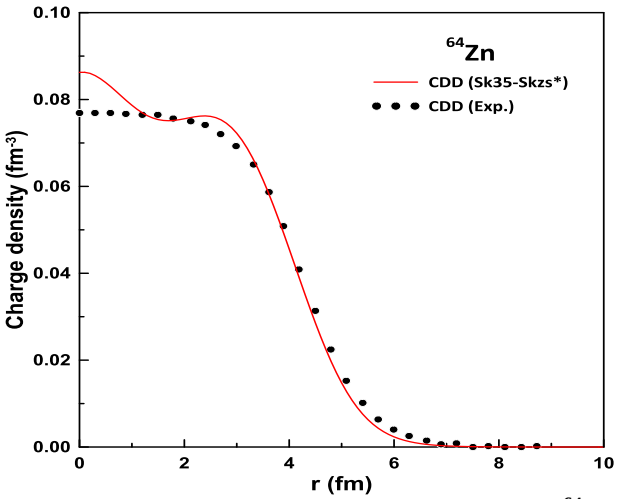

Figure 10. Charge density distribution for ^{64}Zn using Skyrme parameterization "Sk35-Skzs*". Measured data from[21].

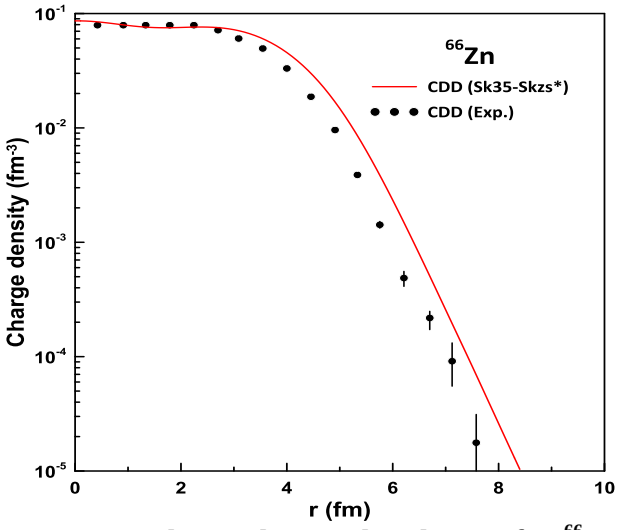

Figure 11. Charge density distribution for ^{66}Zn using Skyrme parameterization "Sk35-Skzs*". Measured data from[22].

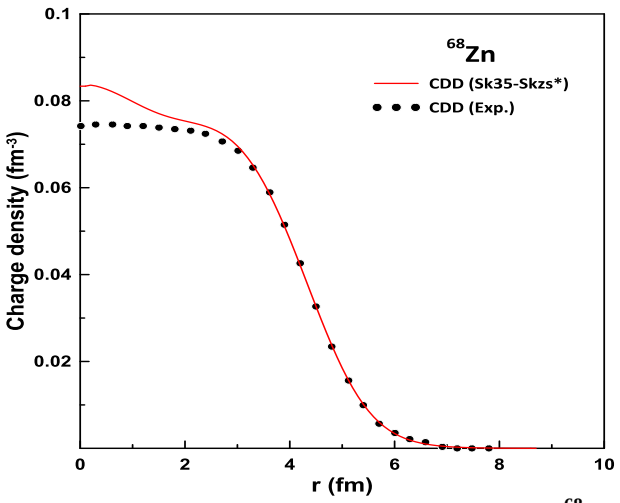

Figure 12. Charge density distribution for ^{68}Zn using Skyrme parameterization "Sk35-Skzs*". Measured data from[23].

Conclusion:

The present study detailed theoretical investigation to study the form factors and charge density distribution (CDD) of inelastic electron scattering for some selected fp-shell nuclei. The theoretical calculations were employed the Skyrme-Hartree-Fock method with (Sk35-Skzs*) parametrization. The comparison of the predicted theoretical values was compared with the available measured data for CDD and C2 form factors and showed good agreement.

Authors' declaration:

- Conflicts of Interest: None.
- We hereby confirm that all the Figures and Tables in the manuscript are ours. Besides, the Figures and images, which are not ours, have been given the permission for re-publication attached with the manuscript.
- Ethical Clearance: The project was approved by the local ethical committee in University of Baghdad.

Authors' contributions:

S.A.A and S.A.E. motivated the idea of the present study. S.A.A. had performed the calculations and both S.A.A. and S.A.E. collaborate to get the experimental data and plot the graphs.

S.H.S and H.M.T wrote the introduction section and the goal of the study.

All the authors participated in discussing and writing the introduction and discussion sections and the conclusions came out from the study.

References:

1. de Forest T, Walecka JD. Electron scattering and nuclear structure. Adv.Phys.1966 Jun;15:1-109.
2. Liu J, Zhang X, Xu C, Ren Z. Theoretical study on nuclear structure by the multiple Coulomb scattering and magnetic scattering of relativistic electrons. Nucl.Phys A 2016. Apr; 948: 46-16.
3. Karataglidis S. Mapping the densities of exotic nuclei. PoS Proc. Sci.2016.Sep; INPC2016. The 26th International Nuclear Physics Conference 11-16 September, 2016, Adelaide, Australia.
4. Hamada T, Johnston, ID. A potential model representation of two-nucleon data below 315 MeV. Nucl. Phys. 1962 Jun; 34:382-21.
5. Kuo TTS, Brown GE. Reaction matrix elements for the 0f-1p shell nuclei. Nucl. Phys. A 1968 Jun; 114: 241-38.
6. Radhi RA, Shell model calculations of inelastic electron scattering for positive and negative parity states in ^{19}F. Nucl. Phys. A 2016 Mar; 947:12-15.
7. Radhi RA, Alzubadi A A, Ali A H. Magnetic dipole moments, electric quadrupole moments, and electron scattering form factors of neutron-rich sd-pf cross-shell nuclei. Phys. Rev. C 2018 Jun; 97: 064312-13.
8. Radhi RA, Alzubadi A A. Study the Nuclear Form Factors of Low-Lying Excited States in ^{7}Li Nucleus Using the Shell Model with Skyrme Effective Interaction. Few-Body Syst. 2019 Aug; 60:57-13.
9. Radhi RA. Calculation of quadrupole transition rates in cross sd-pf shell isotopes (Si, S and Ar). 2nd International Conference on Atomic and Nuclear Physics, November 08-09, 2017 Las Vegas, USA.
10. Majeed FA. The effect of core polarization on longitudinal form factors in ^{10}B. Phys. Scr. 2012 May; 85:065201-4.
11. Majeed FA, Hussain FM. The Role of the core polarization on C2and C4 form factor, Rom. Jour. Phys. 2014 May; 59:95-11.

12. Majeed FA, Obaid SM. Nuclear structure study of ^{22,24}Ne and ^{24}Mg nuclei. Rev. Mex. Fis. 2019Apr;65: 159-9.
13. Hameed BS. The Nuclear Structure for Exotic Neutron-Rich of ^{42,43,45,47}K Nuclei. Baghdad Sci. J. 2020 Apr;13(1):146-9.
14. Skyrme THR. The effective nuclear potential. Nucl. Phys. 1959 Oct; 9:615-20.
15. Ghafouri M, Sadeghi H, Torkiha M. Self-consistent description of the SHFB equations for ^{112}Sn. Results Phys. 2018 Mar;8: 734-10.
16. Baldik R, Dombayci A. Investigation of the production of ^{68}Ga using pre-equilibrium models. Appl. Radiat. Isot., 2016 May; 113:10-7.
17. Sarriguren P, Moreno O, de Guerra E M , Kadrev D N, Antonov A N, and Gaidarov M K. Elastic Magnetic Electron Scattering from odd-A Nuclei. J. Phys.: Conf. Ser. 2020 May; 1555: 012001-8.
18. Brown BA, Rae WDM. The shell-model code NuShellX@ MSU. Nucl. Data Sheets. 2014 Jun; 120: 115-4.
19. Tassie LJ. A Model of Nuclear Shape Oscillations for g-Transitions and Electron Excitation. Aust. J. Phys. 1965 Aug; 9(4): 407-12.
20. Heisenberg J, McCarthy JS, Sick I. Inelastic electron scattering from several Ca, Ti and Fe isotopes. Nucl. Phys. A 1971; 164(2): 353-366.
21. Mooy RBM and Glaudemans PWM. Electron scattering form factors for fp-shell nuclei. Nucl. Phys. A 1971 May; 438: 461-21.
22. Vries HD, Jager CW, De Vries C. Nuclear charge-density-distribution parameters from elastic electron scattering. At. Data Nucl. Data Tables. 1987 Sep; 36:459-41.
23. Fricke G, Bernhardt Heilig CK, Schaller LA, Schellenber LG, Shera EB and De Jager CW. Nuclear Ground State Charge Radii from Electromagnetic Interactions. At. Data Nucl. Data Tables. 1995 Jul; 60:177-108.

استقصاء التركيب النووي لبعض نظائر النيكل والزنك بواسطة تفاعل سكيرم هارتري فوك

شيماء أكرم عباس* سهام حسن سلمان سميرة أحمد أبراهيم هدى مجيد توفيق

قسم الفيزياء، كلية التربية للعلوم الصرفة (أبن الهيثم)، جامعة بغداد، بغداد، العراق.

الخلاصة:

تم التقصي عن عوامل التشكل C2 الغير مرن وتوزيع كثافة الشحنة (CDD) لـ ^{58,60,62}Ni و ^{64,66,68}Zn من خلال استخدام طريقة Skyrme-Hartree-Fock مع معلمات (Sk35-Skzs *). تم حساب عوامل التشكل C2 غير المرن باستخدام شكل نماذج Tassie و Bohr-Mottelson مع الشحنات الفعالة المناسبة للبروتون والنيوترون لحساب مساهمة تأثيرات أستقطاب القلب. تمت مقارنة القيم النظرية المتوقعة مع البيانات المقاسة المتاحة لعوامل الشكل C2 و CDD وأظهرت توافقًا جيدًا جدًا.

الكلمات المفتاحية: توزيع كثافة الشحنة (CDD)، عوامل التشكل C2، سكيرم-هارتري فوك ، نموذج القشرة